Journal of Cerebral Blood Flow and Metabolism
13:24–42 © 1993 The International Society of Cerebral Blood Flow and Metabolism
Published by Raven Press, Ltd., New York

Comparison of Bolus and Infusion Methods for Receptor Quantitation: Application to [^{18}F]Cyclofoxy and Positron Emission Tomography

Richard E. Carson, Michael A. Channing, Ronald G. Blasberg, Bonnie B. Dunn, †Robert M. Cohen, *Kenner C. Rice, and Peter Herscovitch

*Positron Emission Tomography Department, Clinical Center, and *Laboratory on Medicinal Chemistry, National Institute of Diabetes and Digestive and Kidney Diseases, National Institutes of Health, and †Section on Clinical Brain Imaging, Laboratory of Cerebral Metabolism, National Institute of Mental Health, Bethesda, Maryland, U.S.A.*

Summary: Positron emission tomography studies with the opiate antagonist [^{18}F]cyclofoxy ([^{18}F]CF) were performed in baboons. Bolus injection studies demonstrated initial uptake dependent on blood flow. The late uptake showed highest binding in caudate nuclei, amygdala, thalamus, and brainstem and the least accumulation in cerebellum. By 60 min postinjection, regional brain radioactivity cleared at the same rate as metabolite-corrected plasma, i.e., transient equilibrium was achieved. Compartmental modeling methods were applied to time-activity curves from brain and metabolite-corrected plasma. Individual rate constants were estimated with poor precision. The model estimate of the total volume of distribution (V_T), representing the ratio of tissue radioactivity to metabolite-corrected plasma at equilibrium, was reliably determined. The apparent volume of distribution (V_a), the concentration ratio of tissue to metabolite-corrected plasma during transient equilibrium, was compared with the fitted V_T values to determine if single-scan methods could provide accurate receptor measurements. V_a significantly overestimated V_T and produced artificially high image contrast. These differences were predicted by compartment model theory and were caused by a plasma clearance rate that was close to the slowest tissue clearance rate. To develop a simple method to measure V_T, an infusion protocol consisting of bolus plus continuous infusion (B/I) of CF was designed and applied in a separate set of studies. The V_a values from the B/I studies agreed with the V_T values from both B/I and bolus studies. This infusion approach can produce accurate receptor measurements and has the potential to shorten scan time and simplify the acquisition and processing of scan and blood data. **Key Words:** Cyclofoxy—Equilibrium—Infusion—Modeling—Opiate receptor—Positron emission tomography.

Positron emission tomography (PET) researchers have developed many radiopharmaceuticals and analytic strategies with the goal of in vivo quantitation of receptors in humans. Analysis techniques include irreversible and reversible binding models, tissue ratios, equilibrium analyses, linear compartment models applied to tracer doses to assess binding potential, and nonlinear models applied to multiple injection data with varying specific activities or blocking agents for quantitation of B_{max} and K_D (Mintun et al., 1984; Frey et al., 1985*b;* Farde et al., 1986, 1989; Huang et al., 1986, 1989; Perlmutter et al., 1986; Wong et al., 1986*a,b;* Logan et al., 1987; Frost et al., 1989; Salmon et al., 1990; Koeppe et al., 1991; Sadzot et al., 1991). Here, we present our results with the opiate antagonist [^{18}F]cyclofoxy (CF; 6-deoxy-6-β-fluoronaltrexone) for receptor quantitation in baboons with PET.

CF has been extensively characterized in the rat. In vitro studies with [^{3}H]CF demonstrated binding patterns that were nearly indistinguishable from those of [^{3}H]naloxone (Ostrowski et al., 1987).

Received June 4, 1992; final revision received July 20, 1992; accepted July 21, 1992.

Address correspondence and reprint requests to Dr. R. E. Carson at PET Department, Bldg. 10, Rm. 1C-401, NIH, Bethesda, MD 20892, U.S.A.

Dr. R. G. Blasberg's present address is Department of Neurology, Memorial Sloan-Kettering Cancer Center, New York, NY 10021, U.S.A.

Abbreviations used: B/I, bolus plus continuous infusion; CF, cyclofoxy; PET, positron emission tomography; ROI, region of interest.

Rothman and McLean (1988) showed that CF binds to both μ and κ sites. In vivo studies found high extraction fraction and low plasma protein binding (Sawada et al., 1990). In rat and baboon, CF plasma metabolites develop rapidly, but do not cross the blood–brain barrier (Blasberg et al., 1989; Sawada et al., 1991). Compartmental modeling approaches have been applied to kinetic data using varying cold doses to estimate B_{max} and K_D in the rat (Sawada et al., 1991). The inactive enantiomer (+)-CF has been synthesized and shown to have insignificant receptor binding (Rothman et al., 1988). Studies with both enantiomers have permitted regional estimation of nonspecific binding and thereby improved the quality of receptor measurements (Kawai et al., 1990*a,b*). Recently, through the use of double-label infusion studies with [^{3}H](+) − CF *and [^{18}F](−) − CF, simplified methodology has* been developed to measure B_{max} and K_D from true equilibrium studies (Kawai et al., 1991).

Initial PET studies were performed using [^{18}F]acetylcyclofoxy in baboons (Pert et al., 1984; Channing et al., 1985). This form of the tracer was chosen over CF to improve delivery to the brain, based on the relative delivery characteristics of heroin and morphine. However, the rapid deacetylation of this tracer to [^{18}F]CF added substantially to the complexity of the required mathematical model. Once the high permeability of CF was demonstrated, the acetylated form no longer provided any advantage. We now report our initial baboon PET studies with CF and our kinetic modeling approaches.

Ideally, PET modeling efforts lead to a complete, validated model that describes the relationship between PET measurements and the underlying regional physiological parameters, including blood flow, permeability, nonspecific binding, receptor association and dissociation rates, and receptor concentration. With this knowledge, we can design a data acquisition and processing method suitable for human studies (Carson, 1991). Initially, we aim to describe the relationship between the PET data and kinetic parameters to assess what parameter(s) can be reliably and meaningfully estimated.

We present kinetic studies with bolus CF administration analyzed with models using one or two tissue compartments. We also assess whether single-scan measurements provide a useful receptor measure. In particular, do concentration ratios of tissue to metabolite-corrected plasma (apparent volume of distribution) or tissue to nonspecific region provide receptor estimates that agree with model-based methods? Such approaches have the advantages of simplicity of analysis and shortened scan time compared with dynamic studies. Instead of measuring kinetics, scan time can be used to improve image statistical quality and anatomical sampling. In addition, the reduced scanning time can decrease patient discomfort and potentially increase scanner throughput.

We also present compartment theory of receptor binding models, which predicts that the apparent volume of distribution or tissue ratio measures may be significantly affected by the plasma clearance rate. We demonstrate this effect with CF from the analysis of the bolus injection studies. This effect can create differences in ratio measures between patient groups because of differences in plasma clearance, which could be misinterpreted as receptor changes. To circumvent this problem, we devised a tracer administration scheme combining bo*lus injection with continuous infusion (B/I) to pro*duce true equilibrium. The *B/I* protocol was applied in another set of studies and the results compared with the bolus data. With a simple single-scan approach, this infusion method can achieve the accurate quantitation provided by bolus modeling methods.

THEORY

Compartment models for receptor-binding radiotracers

The assumptions and definitions we applied to compartmental models follow those of many other authors (Mintun et al., 1984; Huang et al., 1986; Wong et al., 1986*a;* Frost et al., 1989). Particular details of the model closely adhere to the previous CF work in rats (Blasberg et al., 1989; Kawai et al., 1990a, 1991; Sawada et al., 1991). Owing to the limited statistical quality of PET data, we propose a model that has only two tissue compartments. Compartment 1 (quantity A_1) represents free (A_f) plus nonspecifically bound (A_n) tracer. Compartment 2 (A_2) represents tracer specifically bound to the receptor (A_r). The definitions of the parameters are as follows (symbols are defined in Table 1). The delivery rate constant from plasma to compartment 1 is K_1 (ml/min/ml) and equals the product of blood flow and extraction fraction; k_2 (min^{-1}) defines the rate constant of return from compartment 1 to plasma. We assume that, at true equilibrium, the concentration of free tracer in tissue water equals the concentration in plasma water (Blasberg et al., 1989). In that case, K_1/k_2, which defines the equilibrium ratio of free plus nonspecifically bound tracer to metabolite-corrected plasma CF, equals $f_p\ \omega_T\ (1 + K_{eq})$, where f_p is the fraction of tracer at equilibrium not bound to plasma protein and is measured via ul-

TABLE 1. *Definitions*

A_1	Concentration of tracer in compartment 1 (nCi/cc brain)
A_2	Concentration of tracer in compartment 2 (nCi/cc brain)
A_f	Concentration of free tracer in tissue (nCi/cc brain)
A_n	Concentration of nonspecifically bound tracer in tissue (nCi/cc brain)
A_r	Concentration of tracer specifically bound to receptor in tissue (nCi/cc brain)
A_T	Total concentration of tracer in region of interest (nCi/cc brain)
A'_T	Total concentration of tracer in reference region (nCi/cc brain)
A_v	Concentration of tracer in vascular space (nCi/cc brain)
α_i	Eigenvalues of tissue response (min^{-1})
β	Final plasma clearance rate (min^{-1})
B'_{max}	Free receptor concentration (pmol/ml brain)
B_{max}	Receptor concentration (pmol/ml brain)
C_p	Metabolite-corrected plasma radioactivity concentration (nCi/cc)
C_p^{tot}	Total plasma radioactivity concentration (nCi/cc)
F_{CF}	Fraction of plasma radioactivity that is unmetabolized CF
f_p	Tracer fraction unbound to plasma proteins (ml plasma/ml plasma water)
$h(t)$	General impulse response function
$H(t)$	Infusion schedule
K_1	Rate constant from plasma to tissue compartment 1 (ml/min/ml)
k_2	Rate constant from tissue compartment 1 to plasma (min^{-1})
k_3	Rate constant from tissue compartment 1 to 2 (receptor bound) (min^{-1})
k_4	Rate constant from tissue compartment 2 to 1 (min^{-1})
K_{bol}	Magnitude of bolus in bolus plus continuous infusion protocol (min)
K_D	Equilibrium dissociation constant (n*M*)
K_{eq}	Equilibrium association constant of nonspecific binding (dimensionless)
k_{off}	Dissociation rate constant (min^{-1})
k_{on}	Bimolecular association rate constant ($nM^{-1}\ min^{-1}$)
R_a	Apparent ratio of region of interest to reference region
R_T	Equilibrium ratio of region of interest to reference region
V_a	Apparent total volume of distribution (ml/ml)
V_T	Equilibrium total volume of distribution (ml/ml)
V'_T	Equilibrium total volume of distribution of reference region (ml/ml)
V_v	Effective vascular volume (ml/ml)
ω_T	Water content of tissue (ml water/ml brain)

trafiltration (ml plasma/ml water); ω_T is the water content of tissue (ml water/ml brain), which is assumed to be the distribution space for the receptors; and K_{eq} is the equilibrium association constant for nonspecific binding (A_n/A_f). Although we assume that K_1/k_2 is linearly proportional to f_p, we do not assume that the same is true for the influx rate constant K_1. In other words, the equilibrium between free tracer in plasma and protein-bound tracer may be maintained on a time scale faster than a single capillary transit time. The parameter k_3 is the rate constant of transfer from compartment 1 to 2. Assuming a single receptor system obeying conventional bimolecular kinetics under tracer conditions,

$$k_3 = \frac{k_{on}B'_{max}/\omega_T}{1 + K_{eq}}$$

where k_{on} is the bimolecular association rate constant ($nM^{-1}\ min^{-1}$) and B'_{max} is the concentration of free receptor (pmol/ml brain). The expression B'_{max}/ω_T represents the concentration of receptor in its distribution space (pmol/ml brain water). The parameter k_4 is equal to k_{off}, the dissociation rate from the receptor (min^{-1}). This model assumes one class of specific binding sites, although CF has been shown to bind to both μ- and κ-opiate receptors (Rothman and McLean, 1988). These binding sites may be kinetically indistinguishable, however, at least in rats (Kawai et al., 1991). For regions with no specific binding or where the parameters of the two tissue compartments cannot be identified, a model with one tissue compartment is used. We emphasize that, at this point, we use these models to characterize the kinetic curve. Any physiological meaning ascribed to the parameter estimates of the models must be validated.

Total volume of distribution (V_T)

The concentration ratio between tissue and free tracer in plasma at equilibrium is defined as the total volume of distribution. We chose the free tracer concentration as the reference because it provides a more natural mathematical relationship between V_T and B_{max}. Although true equilibrium is never achieved after a bolus injection, V_T can be estimated from the fitted model parameters by setting all derivatives equal to zero. For the model with two tissue compartments,

$$0 = \frac{dA_1}{dt} = K_1C_p - (k_2 + k_3)A_1 + k_4A_2$$

$$0 = \frac{dA_2}{dt} = k_3A_1 - k_4A_2 \qquad (1)$$

$$V_T = \frac{A_1 + A_2}{f_pC_p} = \frac{K_1}{k_2f_p}\left(1 + \frac{k_3}{k_4}\right)$$

For the one-compartment model,

$$V_T = \frac{K_1}{k_2f_p} \qquad (2)$$

The physiological interpretation of V_T can be derived from equilibrium considerations:

$$V_T = \frac{A_T}{f_p C_p} = \frac{A_f + A_n + A_r + A_v}{f_p C_p}$$

$$= \frac{A_f}{f_p C_p}\left(1 + \frac{A_n}{A_f} + \frac{A_r}{A_f}\right) + V_v$$

where A_v is the radioactivity concentration in the vascular space and V_v is an effective vascular volume (the ratio of the concentration of vascular radioactivity to the concentration of tracer in plasma water). Again assuming that the tracer concentration in tissue water equals that in plasma water at equilibrium, i.e., $A_f/\omega_T = f_p C_p$, then

$$V_T = \omega_T(1 + K_{eq}) + \frac{B'_{max}}{K_D} + V_v \quad (3)$$

where A_r/A_f, the bound-to-free ratio, is equal to the ratio of free receptor concentration (B'_{max}/ω_T) to K_D, assuming tracer conditions. In regions with no specific binding, the equilibrium volume of distribution (V'_T) is

$$V'_T = \omega_T(1 + K_{eq}) + V_v \quad (4)$$

An alternative measure to V_T that is useful when metabolite-corrected plasma is not available is R_T, the concentration ratio between receptor-rich (A_T) and receptor-poor (A'_T) regions:

$$R_T = \frac{A_T}{A'_T} = \frac{V_T}{V'_T} = 1 + \frac{B'_{max}/K_d}{\omega_T(1 + K_{eq}) + V_v}$$

This assumes that the level of nonspecific binding is equal in the two regions.

Transient equilibrium

For reversible ligands, apparent equilibrium can be reached after a bolus injection. This condition occurs when a constant ratio of tissue to blood radioactivity is maintained over time (or a constant ratio between tissue regions). Although radioactivity is clearing from plasma and tissue, the clearance is at the same fractional rate, so a constant ratio is obtained. Following the terminology of parent-daughter decay of radiation physics (Evans, 1955), this condition is defined as "transient equilibrium." V_a, the apparent volume of distribution [$A_T(t)/f_p C_p(t)$], reaches a constant value during transient equilibrium. Ideally, for bolus studies, V_a would equal the ratio at true equilibrium (V_T), and a single scan and a single blood sample could provide receptor information using Eq. 3. However, we demonstrate in Appendix A that during transient equilibrium, $V_a > V_T$. The magnitude of this overestimation depends on the rate of plasma clearance and the local tissue kinetics. A similar error occurs when using the ratio between tissue regions. If R_a is the apparent ratio between a region of interest (ROI) and a reference region with no receptors, i.e., $R_a = A_T(t)/A'_T(t)$, $R_a > R_T$ as well (Appendix A).

Programmed infusion

One approach to measure V_T is to maintain constant blood and tissue concentrations by administering radioactivity as a programmed infusion instead of a bolus. Patlak and Pettigrew (1976) devised a method to generate infusion schedules that can produce various input function forms. Their method has been employed particularly to produce a constant input function. This method has been extended to produce an infusion schedule that rapidly generates constant radioactivity levels in blood and all brain regions to measure the volume of distribution of [^{15}O]water (Carson et al., 1988*a;* Herscovitch et al., 1989). This same approach can be used to produce true equilibrium for receptor studies so that V_T can be measured directly. In this study, we have defined the infusion schedule to consist of a combination of bolus and continuous infusion. The single parameter to be specified in this administration scheme is the magnitude of the bolus (K_{bol}), defined in units of minutes of infusion. For example, a value of 60 for K_{bol} means that the bolus component is equal to 60 min worth of infusion. Appendix B describes the algorithm used to choose an optimum value of K_{bol}.

METHODS

Radiosynthesis of [^{18}F]CF

Aqueous [^{18}F]fluoride (100–150 μl, ~100 mCi) was added to a clean 5-ml V-vial already containing tetramethylammonium hydroxide (30 μl, 30 m*M*). The contents were dried with a stream of argon (block temperature at 100°C), and any residual water was removed by evaporation with anhydrous CH_3CN (3 × 300 μl). To the residue was added the (−)-3-acetyl-6α-naltrexol trifluoromethanesulfonate (2.0 mg, 4 μmol) (Burke et al., 1985) in 400 μl CH_3CN; the vial was capped and the contents were allowed to react at 100°C for 15 min. The vial was cooled, and then with only slight warming, the CH_3CN was concentrated with a stream of argon to ~50–100 μl. The reaction mixture was transferred to a Bond Elut Si Silica cartridge (500 mg; Varian) with 2 × 1 ml $CHCl_3$ and eluted with $CHCl_3/CH_3OH/NH_4OH$ (99:1:0.1). The first 4 ml of eluate was discarded and the next 6 ml, which contained the crude product, collected. The solvent was evaporated with argon at 60°C and the residue dissolved in 125 μl CH_3CN plus 125 μl HPLC eluant (28% CH_3CN/72% 5 m*M* triethylamine/5 m*M* sodium dihydrogen phosphate, pH 3.0, buffer). The crude sample of (−)-3-acetyl-6α-[^{18}F]CF (Channing et al., 1985) was further purified by semipreparative HPLC (Beckman Ultrasphere-ODS, 5 μ, 10.0 × 250 mm). The acetylated 6-[^{18}F]CF was collected (k' = 9.3), and a major portion of the CH_3CN was evaporated with a stream of argon (5 min at 55°C). To this was

added 28% NH_4OH (0.5 ml); the mixture was vortexed and heated at 55°C for 3 min. The mixture was applied to a C_{18} octadecyl Bond Elut cartridge (500 mg; Varian), which had previously been rinsed with 10 ml each of ethanol and water. The cartridge was rinsed with 10 ml water. The 6α-[^{18}F]CF was eluted with 2 ml absolute ethanol, and the ethanol was evaporated. The product was formulated by sequential addition and thorough mixing of 100 μl ethanol, 100 μl 2 N acetic acid, and 10 ml 3.8% (wt/vol) sodium citrate for injection (NIH Pharmaceutical Development Service) and sterilized by filtration through a 25-mm, 0.22-μm filter (Millex-GV; Millipore). The yield of final product was 38.5 ± 5.9% and the measured radioactivity averaged 17.6 ± 8.8 mCi (n = 8, decay corrected to end of bombardment). The total synthesis time was 100 min. The specific activity (at end of bombardment) averaged 10.7 ± 8.8 Ci/μmol (n = 8), and both chemical and radiochemical purity were >98% as determined by HPLC (Beckman Ultrasphere-ODS, 5 μ, 4.6 × 250 mm, 30% CH_3CN/70% 5 m*M* triethylamine/5 m*M* sodium dihydrogen phosphate, pH 3.0, buffer).

Animal studies

Eight PET studies were performed in laboratory-bred male baboons (*Papio* sp.) ranging in weight from 15 to 25 kg. Animals were anesthetized intramuscularly with ketamine, typically 10 mg/kg every 30 min. Endotracheal intubation was performed for control of respiration, an intravenous line was inserted in a distal lower extremity, and a femoral artery catheter was inserted on the contralateral side by either percutaneous puncture or cut-down and sutured in place. The animals were transported to the PET suite and were positioned on the scanning table. Prior to and during scanning, Pavulon (0.03 mg/kg i.v. every 90 min) was administered to paralyze the animals. Blood pressure, temperature, and ECG were continuously monitored. Ventilation was controlled with a Bennett ventilator, end-tidal P_{CO_2} was continuously monitored, and arterial blood gases were serially sampled. A thermoplastic mask was fitted to the animal's head to maintain its position in the scanner. All studies were performed under a protocol approved by the NIH Clinical Center Animal Care and Use Committee.

Administration of CF

Four studies were performed with bolus administration, and four studies used a combination of bolus plus continuous infusion (B/I). For bolus studies, 4–7 mCi of CF was administered intravenously over a 1-min period. This period was chosen to reduce sensitivity to errors in blood sampling. In the B/I studies, a computer-controlled pump (Harvard model 22, South Natick, MA, U.S.A.) was used to ensure accurate and reproducible administration of radioactivity. The dose was diluted with saline to a total volume of 50 ml. The bolus fraction of the dose (plus sufficient volume to fill the catheter dead space) was administered at the pump's highest speed (26 ml/min). Pump speed was changed by computer at the appropriate time to administer the remaining dose uniformly. In one B/I study, the infusion was purposely interrupted after 70 min to alter plasma clearance, and scanning was continued until 120 min. In two studies, the infusion continued until 120 min. One study was terminated at 60 min.

Blood sampling and metabolite determination

Following CF administration, 1-ml arterial blood samples were withdrawn at the following times: 0:15, 0:30, 0:45, 1, 1:15, 1:30, 1:45, 2, 2:30, 3, 4, 5, 7, 10, 15, 20, 30, 40, 50, 60, 75, 90, and 120 min. Samples were centrifuged, and 0.3 ml of plasma was counted in a calibrated gamma counter. At least 12 samples were analyzed by an ethyl acetate extraction procedure to determine the fraction of radioactivity representing unmetabolized CF (Kawai et al., 1990*b*). This procedure has been validated against HPLC measurements in rat and baboon plasma (Blasberg et al., 1989; Sawada et al., 1991). A 100-μl aliquot of plasma was added to 300 μl of borate buffer (pH 9.0; 0.2 m*M*) followed by 400 μl of ethyl acetate. The sample was vortexed (>10 s) and centrifuged at 13,000 *g* for 1 min. Samples of the organic and aqueous phases were pipetted (200 μl) and counted in a gamma counter. The fraction of unmetabolized CF (F_{CF}) was determined from the ratio $C_o/(C_o + C_a)$, where C_o and C_a are the concentrations in the organic and aqueous phases, respectively. The fractions were normalized to the extraction efficiency of this procedure, which was determined by a sample consisting of ~5 μCi of CF added to 5 ml of nonradioactive blood. The efficiency was 96.2 ± 0.8% (SD). After deletion of outliers, data were smoothed by fitting overlapping five-point segments to quadratic polynomials. A continuous curve was passed through these points using cubic splines (Carson et al., 1981). The metabolite-corrected CF input function (C_p) was calculated from the product of the F_{CF} curve and the total plasma radioactivity (C_p^{tot}).

The fraction of CF in plasma bound to plasma proteins was determined by ultrafiltration (Sawada et al., 1990). 300 μl of plasma from the sample used to measure ethyl acetate efficiency was applied to a Centrifree microparti tion membrane (Amicon, Danvers, MA, U.S.A.) and centrifuged for 15 min at 2,000 *g*. The free fraction in plasma (f_p) was calculated from C_u/C_p, where C_u is the concentration in the ultrafiltrate (nCi/ml plasma water). This procedure was not performed in the initial studies described here. Therefore, a mean f_p value calculated from the remaining studies and from another series of CF studies (Carson et al., 1989) was applied in the calculations. Measured f_p values were 0.7456 ± 0.0264 ml plasma/ml plasma water (n = 11).

PET scanning procedure

Scans were performed with the Scanditronix PC1024-7B brain tomograph (Daube-Witherspoon et al., 1987) which acquires seven simultaneous slices, 13.75 mm apart. Reconstructed in-plane resolution is 6.5 mm, and axial resolution is 10–12 mm. The baboons were positioned so that slices were parallel to the orbitomeatal line. Transmission scans were acquired with either a rin source or a rotating rod source. Dynamic scans were acquired beginning with tracer arrival in the brain. Image reconstruction included corrections for attenuation, scatter, randoms, and deadtime. Pixel values were calibrated in nanocuries per cubic centimeter with a uniform phantom filled with ^{18}F. The baboon brain was visible in three to four adjacent slices. Images were summed from 0 to 60 min post injection and 60 to 120 min to improve statistics for the purpose of identifying ROIs. Slices were matched to a baboon brain atlas (Riche et al., 1988) and ROIs (circular and irregular) of size 1–4 cm^2 (4 mm^2/pixel) were placed on the images. Regions were drawn on both hemispheres on the cerebellum, frontal, temporal, and parietal cortex (two levels), caudate nuclei, amygdala, and white matter (centrum semiovale). Single midline regions were drawn for occipital cortex and thalamus.

Data analysis

Decay-corrected time-activity curves were fit to three different models. Model 1 included two serial tissue compartments and four parameters and is described mathematically by Eqs. A1, A10, and A11 of Appendix A. To minimize errors due to vascular radioactivity and time shifts between brain and blood measurements, data collected before 3 min post injection were not used with model 1. Model 2 is a five-parameter model, which includes a term for vascular radioactivity of the form $V_pC_p^{tot}$ and was applied to scan data beginning at injection time. Model 3 is a reduced model consisting of one tissue compartment plus vascular radioactivity and has three parameters (K_1, k_2, V_p). In the implementation of all models, the input function is considered to be piecewise linear between sample points, and the tissue model includes integration over each scan interval. Parameter estimates are derived by weighted nonlinear regression, where weights are chosen as the inverse of the variance of the ROI value determined by Budinger's formula (Budinger et al., 1978) modified to account for region size and random counts. The covariance matrix of the parameter estimates, produced by the fitting procedure, is used to calculate standard errors of functions of the rate constants including V_T. The quality of the fits to models 1–3 was compared using the Akaike information criterion (*AIC;* Akaike, 1976):

$$AIC = n \ln(WSS) + 2p$$

where n is the number of data points, WSS is the weighted sum of squares, and p is the number of parameters. Parameter estimates for bilateral ROIs were averaged.

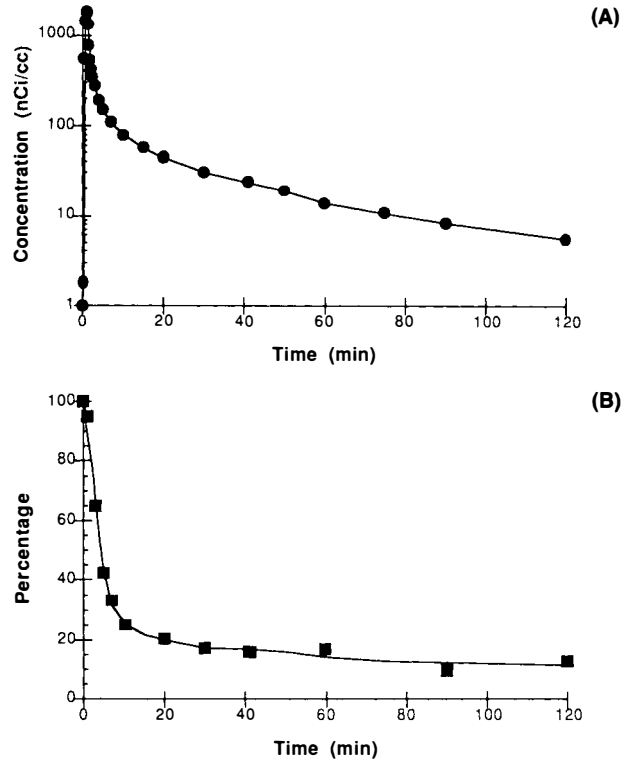

FIG. 1. A: Total radioactivity in plasma after bolus administration of cyclofoxy (CF) (log scale). **B:** Percentage of plasma radioactivity that is unmetabolized CF (extracted in ethyl acetate). Solid line is spline fit used for modeling. See text for details.

RESULTS

Bolus studies

Typical plasma time-activity data after a bolus CF injection are shown in Fig. 1. Figure 1A depicts total radioactivity, which dropped rapidly, with a clearance rate of 1.4 ± 0.4%/min (n = 4) from 20 to 120 min post injection. Figure 1B shows the percentage of that radioactivity that was extracted in ethyl acetate: 40.8 ± 5.7% at 5 min, 25.8 ± 2.8% at 10 min, 21.1 ± 1.7% at 20 min, 13.7 ± 1.3% at 60 min, and 11.9 ± 2.2% at 120 min (n = 4).

These studies used high specific activity CF (>1 Ci/μmol). By 20 min post injection, the plasma concentration of free CF was below 10 nCi/cc, resulting in a cold concentration of <0.01 n*M*. With measured K_D values of 0.34–1.5 n*M* in vitro (Rothman and McLean, 1988) and 1–2 n*M* in vivo (Kawai et al., 1991), and assuming that the free tissue CF concentration is comparable with that in plasma, there was essentially no change in receptor occupancy caused by the injected CF. The peak tissue concentration was 1,000 nCi/cc or <1 n*M*. Even assuming that 100% of the radioactivity was receptor bound, <10% of the receptors would be occupied based on in vitro and in vivo B_{max} values (Rothman and McLean, 1988; Kawai et al., 1991).

Images from a bolus injection study are shown in Fig. 2. The top row of images are averages of scans collected 0–10 min post injection. They portray a radioactivity distribution very similar to that seen in cerebral blood flow studies with [^{15}O]water (data not shown). The late images, which are produced by averaging scans from 60 to 120 min post injection, show a markedly different radioactivity pattern. The highest accumulation of tracer occurred in caudate nuclei, amygdala, thalamus, and brainstem, while the least accumulation occurred in cerebellum. High uptake can also be seen in the pituitary.

Sample tissue time-activity curves for the study depicted in Figs. 1 and 2 are shown in Fig. 3A. The data peak ~5 min post injection and then decline rapidly. Transient equilibrium between tissue regions and plasma is assessed by plotting the apparent volume of distribution (V_a) versus time (Fig. 3B). A constant ratio of tissue to metabolite-corrected plasma is reached by 10 min in cerebellum, the region with lowest binding. Constant V_a is reached at later times for regions with higher binding.

Models 1, 2, and 3 were applied to all ROIs. The means and standard deviations of rate constants de-

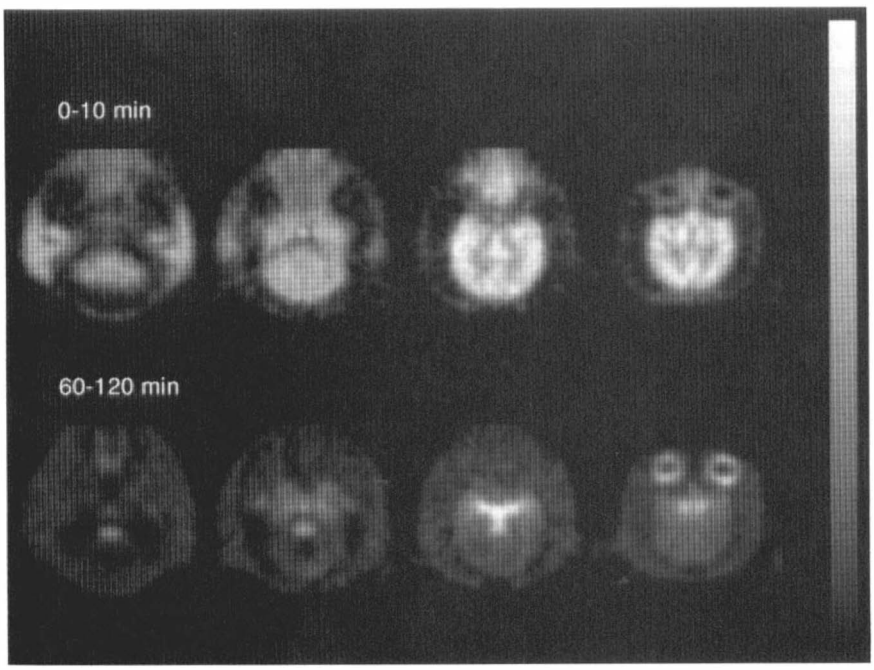

FIG. 2. Images from cyclofoxy bolus injection study (same study as in Fig. 1). **Top:** Cross-sectional images, 13.75 mm apart, created by averaging data from 0 to 10 min post injection. Images are displayed on common scale of 0–1,000 nCi/cc. **Bottom:** Images from same levels obtained by averaging data from 60 to 120 min post injection. Images are displayed on common scale of 0–500 nCi/cc.

rived from model 1 (four-parameter model) are presented in Table 2. Figure 3A shows examples of the quality of fits obtained using model 1. The K_1 values are quite high, consistent with a lipophilic tracer with low protein binding (Fenstermacher et al., 1981). The k_4 values, presumably k_{off}, were reasonably uniform across brain regions and had lower variability among animals in regions with high binding. The estimates for k_2 and k_3, however, are highly variable. Ideally, k_3 values would reflect free receptor concentration; i.e., the highest values would be in regions with highest binding. This was not the case. Instead, this model tended to produce estimates of k_2 that were lower in the regions with higher total binding. The volume of distribution for free plus nonspecifically bound tracer (K_1/k_2f_p) ranges from 4 to 9 ml/ml in cerebellum and cortical regions and from 11 to 16 ml/ml in thalamus, amygdala, and caudate. This model-based estimate of free plus nonspecific binding disagrees with measured values using the inactive enantiomer (+)-CF in both rats and baboons (Carson et al., 1989; Kawai et al., 1990*a*). In baboons, the (+)-CF volume of distribution was 6–8 ml/ml for all brain regions (after correction for f_p), and regions with higher specific binding did not have higher nonspecific binding. Although the quality of the fits is quite good, the estimated parameter values are not consistent with their conventional physiological interpretation.

Even though individual parameter values were highly variable, the total volume of distribution (Eq. 1), a parameter sensitive to receptor concentration

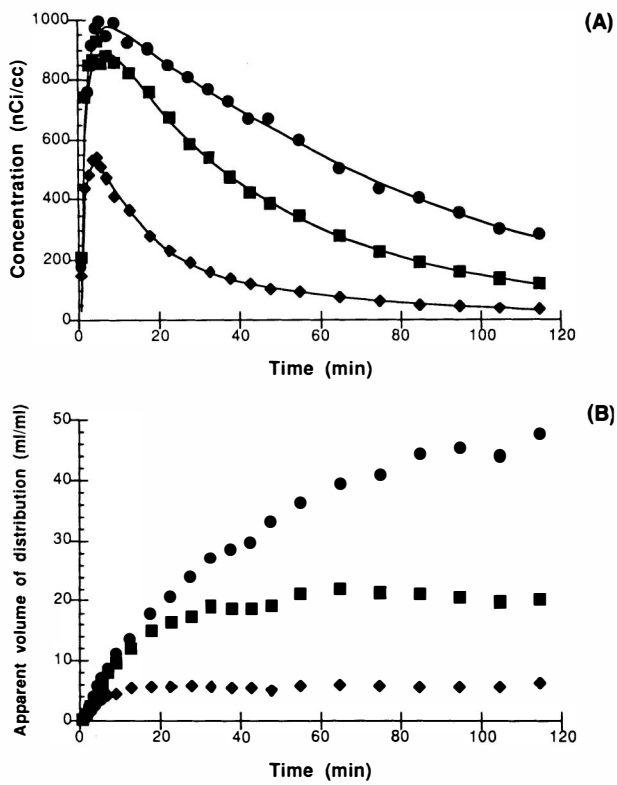

FIG. 3. A: Tissue time-activity data from positron emission tomography images for thalamus (●), frontal cortex (■), and cerebellum (♦). Same study as in Figs. 1 and 2. Frontal cortex and cerebellum curves are averages of left and right regions. All data are decay corrected to time of injection. Solid line is result of best fit to each curve. **B:** Apparent volume of distribution (V_a; ratio of tissue activity to metabolite-corrected plasma activity) for regions from A.

TABLE 2. *Cyclofoxy rate constants*

Region	K_1 (ml/min/ml)	k_2 (min^{-1})	k_3 (min^{-1})	k_4 (min^{-1})
Amygdala	0.427 (0.078)	0.051 (0.013)	0.030 (0.020)	0.033 (0.011)
Caudate nuclei	0.530 (0.111)	0.047 (0.011)	0.028 (0.028)	0.039 (0.012)
Cerebellum	0.374 (0.045)	0.123 (0.021)	0.016 (0.027)	0.036 (0.055)
Frontal cortex	0.578 (0.083)	0.169 (0.220)	0.121 (0.217)	0.045 (0.022)
Occipital cortex	0.605 (0.063)	0.108 (0.030)	0.020 (0.027)	0.052 (0.041)
Parietal cortex	0.560 (0.075)	0.120 (0.052)	0.079 (0.137)	0.064 (0.063)
Temporal cortex	0.390 (0.066)	0.077 (0.040)	0.037 (0.082)	0.043 (0.031)
Thalamus	0.519 (0.020)	0.082 (0.042)	0.063 (0.068)	0.033 (0.017)
White matter	0.374 (0.077)	0.073 (0.015)	0.016 (0.015)	0.038 (0.016)

Values are means (SD) of rate constants derived from fit of data between 3 and 120 min post injection in four bolus injection studies using model 1 (four parameters, two tissue compartments).

(Eq. 3), was estimated with much higher accuracy. For example, the mean coefficients of variation (ratio of the parameter's standard error to its value) for model 1 were as follows: K_1, 6.6%; k_2, 21.4%; k_3, 58.2%; k_4, 26.0%. For V_T, the coefficient of variation was typically 1–2%. Since V_T can be estimated by all three models, values were chosen from the model that provided the best fit, as determined by the lowest *AIC*. Occasionally, however, the *AIC* chose a fit that estimated V_T with a substantially larger standard error. Therefore, to ensure that V_T was estimated reliably, a model with a lower *AIC* was not selected as the best fit if its predicted standard error of V_T exceeded that of model 3 by >10%. Of the 72 ROIs analyzed (18 per animal), model 3 converged in all instances. Convergence did not occur for six ROIs for model 1 and for a different set of six ROIs for model 2. Convergence failures were not associated with any particular brain region. The best fits were determined to be for model 1, 64 ROIs; for model 2, 5 ROIs; and for model 3, 3 ROIs. The V_T values and their standard deviations are tabulated in Table 3 for fits of 120 min of data. In the 64 ROIs with best fit using model 1, the V_T values from model 3 consistently underestimated the model 1 values (mean difference: 0.98 ± 0.58 ml/ml) with a correlation coefficient of 0.993 and a linear regression of

$$V_T \text{ (model 3)} = 0.934 \times V_T \text{ (model 1)} - 0.38$$

The V_T values varied over a 5:1 range, with the highest total binding in caudate nuclei, amygdala, and thalamus, intermediate binding in cortical areas, and lowest binding in cerebellum. This binding order is consistent with the in vitro distribution of opiate receptors in primates (Lewis et al., 1981). The coefficient of variation across animals ranged from 8 to 23%. If nonspecific binding is assumed to be uniform and cerebellar binding is considered to be predominately nonspecific, then specific binding accounts for 75–80% of V_T in receptor-rich regions and 50–60% of V_T in cortical regions. Resolution limitations certainly affect these values, both in the small receptor-rich regions (caudate, amygdala) and in regions such as cerebellum, owing to transverse and axial partial volume effects (Hoffman et al., 1979; Kessler et al., 1984).

To assess the stability of the V_T estimates, fits to just the first 60 min of each data set were performed. In this case, convergence did not occur for 24 ROIs for model 1 and 13 ROIs for model 2. The

TABLE 3. *Total volume of distribution (ml/ml): bolus studies*

Region	V_T (0–120 min)	V_T (0–60 min)	V_a (60–120 min)	V_a (40–60 min)
Amygdala	20.75 (2.91)	18.16 (2.18)	49.11 (15.53)	38.53 (13.40)
Caudate nuclei	24.71 (5.46)	22.34 (3.32)	52.84 (9.05)	44.46 (8.67)
Cerebellum	5.26 (0.57)	4.81 (0.63)	8.07 (0.96)	7.91 (0.76)
Frontal cortex	14.11 (1.16)	13.04 (0.99)	25.83 (4.04)	25.93 (3.26)
Occipital cortex	9.75 (1.38)	8.68 (0.60)	14.32 (3.67)	15.90 (3.76)
Parietal cortex	9.77 (0.29)	9.00 (0.70)	14.88 (1.91)	16.01 (1.56)
Temporal cortex	10.45 (2.53)	9.52 (1.88)	18.76 (4.96)	18.66 (2.63)
Thalamus	20.23 (2.55)	19.56 (3.38)	47.79 (13.73)	39.33 (11.73)
White matter	9.36 (1.16)	8.69 (0.62)	17.06 (3.70)	17.20 (2.64)

Mean (SD) total distribution volume values for bolus injection studies. V_T values determined from best fit of data from 0 to 120 or 0 to 60 min. See text for details of models and choice of best fit. V_a, the apparent volume of distribution, is determined by the ratio of average tissue activity to average metabolite-corrected blood activity from 60 to 120 and 40 to 60 min. All values have been adjusted for plasma free fraction.

best-fit totals were as follows: model 1, 30 ROIs; model 2, 14 ROIs; model 3, 28 ROIs. There was no relationship between regions and the choice of best fit. The best-fit V_T values for the 60-min fits are listed in Table 3. The 60-min V_T values underestimated the 120-min values (mean difference: 0.80 ± 0.99 ml/ml). The correlation coefficient was 0.979 and the linear regression was

$$V_T\,(60\text{ min}) = 0.878 \times V_T\,(120\text{ min}) + 0.333$$

Part of this difference is due to the selection of model 3 for 28 ROIs for the 60-min fits.

The measured ratios of tissue to metabolite-corrected plasma (V_a) are listed in Table 3, where data were averaged from 60 to 120 and from 40 to 60 min post injection. The early and late V_a data are in good agreement, except in high binding regions (amygdala, caudate nuclei, and thalamus) where transient equilibrium has not yet been completely achieved by 40 min. Comparison with V_T values shows a substantial overestimation by V_a, as predicted in Appendix A. In other words, the concentration ratio of tissue to plasma is an incorrect measure of receptor because of its sensitivity to the plasma clearance rate. Figure 4A shows the relationship between V_a (60–120 min) and V_T (120-min best fit). Their correlation is 0.95 and the linear regression is

$$V_a = 2.53 \times V_T - 7.53$$

In high binding regions, V_a exceeds V_T by 80–200%, while the overestimation is 20–120% for lower binding regions. This relationship is consistent with Eqs. A13 and A14 (see Appendix A), which predict larger overestimation for regions with smaller values of α_1 (the slowest tissue clearance rate). The correlation between α_1 (Eq. A11) and V_T was −0.79. Also, the coefficient of variation of V_a is larger than that of V_T.

The ratio of regional radioactivity to that in a region with low binding (R_a) is an alternative measure of receptor to V_a. The relationship of R_a to R_T is shown in Fig. 4B, where cerebellum is used as the nonspecific region. Again, R_a exceeds R_T. The correlation of R_a and R_T is 0.96 and the linear regression is

$$R_a = 1.68 \times R_T - 1.02$$

The errors are smaller than those with V_a because there is some cancellation of errors due to overestimation in the reference region (Eq. A16).

B/I studies

With use of the bolus study results, a B/I administration scheme was determined (Appendix B). For

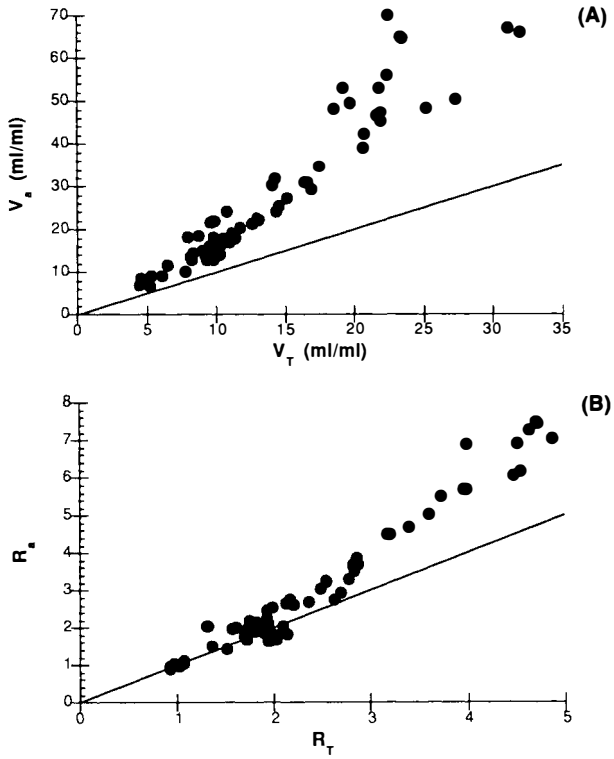

FIG. 4. A: Relationship between apparent volume of distribution (V_a) calculated from 60 to 120 min post injection and fitted total volume of distribution (V_T) for bolus injection studies. Each data point represents 1 of 18 regions in each of four animals. Solid line is line of identity. **B:** Apparent tissue ratio values (R_a) vs. fitted values (R_T) for bolus studies. Values represent ratios of regional values to average of left and right cerebellum values.

each animal, the time-activity curves in plasma, cerebellum, and thalamus were used to determine the bolus portion of the dose (K_{bol}). The mean value was 75.1 ± 9.0 min (n = 4). An example of the predictions of the optimization is shown in Fig. 5 for the baboon whose data were shown in Figs. 1–3. The predicted curves for plasma (Fig. 5A), thalamus (Fig. 5B), and cerebellum (Fig. 5C) are shown for K_{bol} values of 50, 75, and 100 min. The optimization chose a K_{bol} value that produced a constant level for all curves at similar times. For example, a lower K_{bol} value of 50 produced more rapid plasma equilibrium but slower equilibrium in the thalamus.

Four B/I studies were performed. In one study, in the same animal whose data are shown in Figs. 1–3, the infusion was interrupted at 70 min post injection. The purpose of this interruption was to demonstrate with measured data the sensitivity of V_a to the plasma clearance rate. Figure 6 shows the results of this study. Radioactivity in the plasma (Fig. 6A and B) and tissue regions (Fig. 6C) reached steady levels by 20 and 30 min, respectively. At 70 min post injection, the infusion was discontinued,

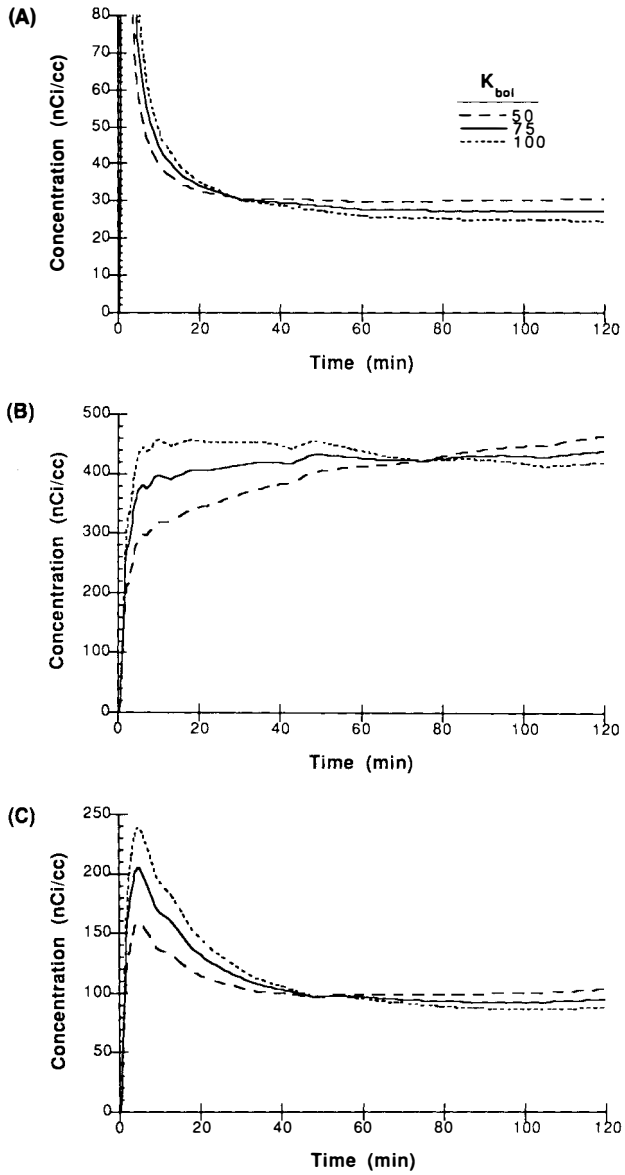

FIG. 5. Predicted results of bolus plus continuous infusion studies for three different magnitudes of bolus: K_{bol} = 50, 75, and 100 min. Curves are calculated from Eq. B2 using the measured data from the study shown in Figs. 1–3. **A:** Metabolite-corrected plasma activity; **B:** thalamus; **C:** cerebellum.

and plasma and tissue concentrations dropped. The unmetabolized fraction of CF in plasma also dropped to levels similar to that in the bolus studies. Figure 6D shows the apparent volume of distribution (V_a) plotted against time. Discontinuing the infusion caused a dramatic increase in V_a in thalamus and smaller increases in frontal cortex and cerebellum. This change is due solely to the change in clearance from plasma and demonstrates that V_a can be significantly affected by plasma clearance. It is interesting to note that the entire 120 min of data of this study can be fitted well with model 1 (Fig. 6C).

The B/I infusion protocol was applied in three additional studies. Sample results are shown in Fig. 7. The average plasma clearance rate was +0.06 ± 0.12%/min from 20 to 60 min. The unmetabolized fraction in plasma was 25.9 ± 11.9% at 20 min and 26.0 ± 10.5% at 60 min, substantially higher than the comparable values from the bolus studies. The mean tissue clearance rates from 20 to 60 min were −0.27 ± 0.38%/min in thalamus, +0.21 ± 0.29%/min in frontal cortex, and +0.38 ± 0.35%/min in cerebellum. This pattern is similar to the predicted curves of Fig. 5, which show a small rise in thalamus (negative clearance rate) and a small downward trend in frontal cortex and cerebellum. The time-activity data were fit to the three models, the best fits were determined, and the resulting V_T values are tabulated in Table 4 for fits of 0–120 min (n = 2) and for 0–60 min (n = 4). The mean percentage differences (across ROIs) between V_T values from the infusion studies and the bolus studies (0–120 min) were 3.8 ± 15.4% (120-min fits) and 4.1 ± 12.5% (60-min fits).

Figure 8A compares the best-fit V_T values (60-min fits) with the values for the apparent volume of distribution averaged from 40 to 60 min in an analogous manner to Fig. 4A. V_T and V_a had a correlation coefficient of 0.96 and a linear regression of

$$V_a = 0.88 \times V_T + 1.18$$

The pattern of slight underestimation of V_T for low binding regions and slight overestimation for high binding regions is consistent with the predictions of the simulation studies (Fig. 5B and C). When the V_a data from 60 to 120 min are compared with matching V_T estimates, the correlation coefficient is 0.95 and the linear regression is

$$V_a = 1.05 \times V_T - 0.41$$

although this includes data from only two studies. There is much better agreement between V_a and V_T for the B/I studies than for the bolus studies (Fig. 4A). The mean percentage difference (across regions) between V_a values from infusion studies (40–60 min) and V_T values from bolus studies (120-min fits) was 5.8 ± 14.7%. Figure 8B shows the relationship between the apparent tissue ratios (R_a) and the fitted values (R_T). Agreement is similarly much better than the bolus study results (Fig. 4B).

DISCUSSION

The primary goal of this study is to evaluate methods to obtain reliable and physiologically meaningful receptor measurements with [^{18}F]CF and PET and to specify a suitable protocol for hu-

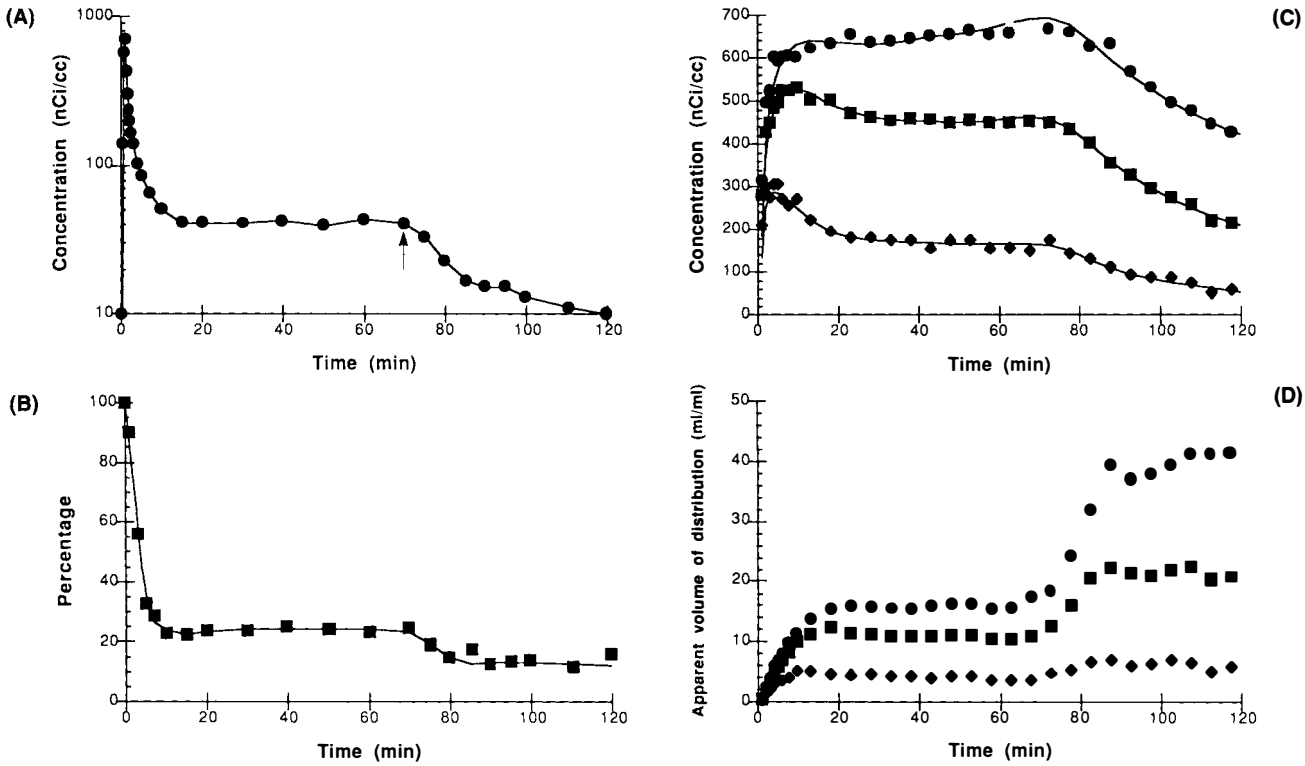

FIG. 6. Discontinued infusion study. Cyclofoxy (CF) was administered according to the bolus plus continuous infusion protocol, but the infusion was discontinued at 70 min (arrow). Same animal as in Figs. 1–3, studied on a different day. **A:** Total plasma radioactivity; **B:** percentage of unmetabolized CF in plasma with spline fit; **C:** tissue time-activity data for thalamus (●), frontal cortex (■), and cerebellum (♦) with best-fit curves (solid lines); **D:** apparent volume of distribution (V_a) as a function of time for regions in C.

man studies. The extensive evaluation of CF in the rat provided an excellent basis for the development of modeling methodology. However, the considerable differences between PET data and autoradiographic or tissue-sampling measurements, as well as the species differences between rodents and primates, may limit the applicability of the information obtained in the rat experiments. For example, PET studies allow acquisition of multiple time points in a single study, avoiding interindividual variability. However, the spatial resolution and statistical reliability of PET data are substantially worse than in rat measurements. Therefore, kinetic parameters that can be reliably measured in rat studies may not be numerically identifiable from PET data.

Conventional compartment modeling and parameter estimation

The time-activity data after bolus injections were analyzed using compartmental modeling techniques. Model 1 included two tissue compartments and was applied to data acquired after 3 min post injection to avoid the effects of vascular radioactivity. Model 2 added vascular radioactivity and was applied to the full data set. Note that because of the high permeability of CF, vascular radioactivity should not introduce significant errors, since the venous drainage rapidly equilibrates with the free pool in tissue. However, the presence of radioactive metabolites at later times will slightly bias the results from model 1. Model 3 (one tissue compartment plus vascular radioactivity) was originally included for fits to regions with little or no specific binding. Ideally, reliable parameter estimates could be obtained in receptor-rich regions using models 1 or 2. These parameter estimates would in theory allow direct measurement of delivery, nonspecific binding, the binding potential, and receptor dissociation rate. Although convergence could be achieved for most ROIs, and model 1 was found to be most suitable according to the Akaike information criterion, the model 1 parameter estimates were variable across animals and the values were not consistent with their expected physiological interpretation. The ratio K_1/k_2f_p, the equilibrium distribution volume for free plus nonspecifically bound tracer, showed a wide variation across regions, with higher values in receptor-rich areas. This result conflicts with studies of the inactive enantiomer (+)-CF in rats and baboons (Carson et al., 1989;

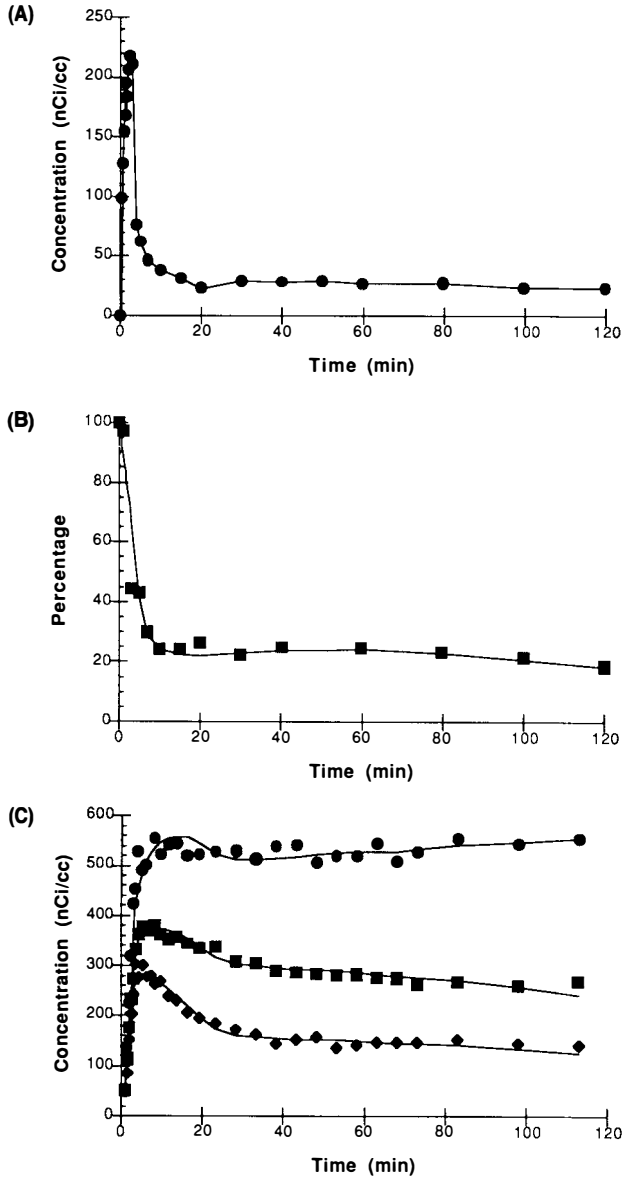

FIG. 7. Results of 120-min bolus plus continuous infusion study. **A:** Total plasma radioactivity; **B:** percentage of unmetabolized cyclofoxy in plasma with spline fit; **C:** tissue time-activity data for thalamus (●), frontal cortex (■), and cerebellum (♦) with best-fit curve (solid line).

Kawai et al., 1990*a*), which showed lower nonspecific binding levels and smaller nonuniformities.

There are many possible reasons why the model 1 estimates are not consistent with physiological expectations. The presence of binding to two receptor sites poses a problem, but this did not limit the use of even more complex kinetic models with rat data (Sawada et al., 1991). Primarily, there is low sensitivity to the parameters k_2 and k_3 in the measured data, as seen by their large standard errors. Usually, standard errors are a lower bound on the true variability of the results, because of error sources that are not included in the model (Carson, 1991). In addition, there are biases introduced in the fits owing to effects such as uncorrected scatter in the tissue data, errors in metabolite corrections, and time shifts between brain and plasma data. These effects can significantly alter parameter values, particularly when sensitivity to the parameters is low. When only 60 min of data was used, best fits to models 1 or 2 could be achieved for only 60% of the regions. These results suggest that, without additional constraints, it is highly unlikely that individual parameters can be reliably estimated in human studies, particularly considering the reduced statistical image quality (due to dosimetry considerations) and additional variability introduced by patient motion.

One approach to improve precision is to limit the number of floating variables. For example, because of the high extraction of CF, K_1 could be estimated from measured blood flow values and an assumed value for PS. Alternatively, the nonspecific binding level could be estimated from a region with little or no binding. For example, Frost et al. (1989) used parameters from occipital cortex fits to limit the number of floating parameters in fits of high binding regions. Another method is to use an inactive enantiomer that can properly account for regional variations in nonspecific binding, but requires an additional study. These techniques are useful to extract the most information possible from PET kinetic data. Validation studies, however, are necessary to verify the accuracy of the assumptions and assess the magnitude of propagation of errors (Huang and Phelps, 1986; Carson, 1991).

The parameter that is most reliably estimated from kinetic data is V_T, the total volume of distribution. V_T should equal the concentration ratio of tissue to free, metabolite-corrected plasma at true equilibrium. V_T is a measure of receptor concentration (Eq. 3), has small variability, and is, to a great extent, model independent. V_T can be estimated by models 1, 2, or 3. The robustness of this measure is shown, to some extent, by the good agreement between 60- and 120-min fits and between the different model fits. There is a small bias in the model 3 values compared with model 1. Part of this difference is due to vascular metabolites, which are not included in model 1 and will cause a slight overestimation of V_T. The difference, V_v (Eq. 3), is the ratio of vascular radioactivity (nCi/ml brain) to the CF concentration in plasma water and can be approximated as

$$V_v = \frac{A_v}{f_p C_p} \cong \frac{V_b C_p^{tot}}{f_p C_p} = \frac{V_b}{f_p F_{CF}}$$

TABLE 4. *Total volume of distribution (ml/ml): infusion studies*

Region	V_T (0–120 min)	V_T (0–60 min)	V_a (60–120 min)	V_a (40–60 min)
Amygdala	18.76 (3.88)	18.57 (2.54)	18.74 (6.47)	17.61 (3.06)
Caudate nuclei	24.67 (3.07)	23.83 (5.53)	24.55 (8.6)	22.29 (5.35)
Cerebellum	6.87 (0.01)	6.35 (0.56)	7.28 (0.95)	6.91 (0.99)
Frontal cortex	13.62 (0.93)	14.81 (0.70)	14.08 (0.61)	15.08 (2.02)
Occipital cortex	7.62 (0.83)	8.23 (0.97)	7.99 (0.02)	9.23 (1.63)
Parietal cortex	10.19 (0.09)	10.52 (0.72)	10.60 (1.13)	11.09 (1.12)
Temporal cortex	12.41 (2.06)	12.45 (2.40)	13.21 (3.82)	12.57 (2.81)
Thalamus	22.52 (3.00)	22.77 (1.96)	23.12 (8.98)	21.76 (4.66)
White matter	9.74 (1.86)	9.49 (1.51)	9.91 (3.42)	9.66 (1.90)

Mean (SD) total distribution volume values for infusion studies. V_T values determined from best fit of data from 0 to 120 (n = 2) and 0 to 60 (n = 4) min. See text for details of models and choice of best fit. V_a, the apparent volume of distribution, is determined from 60 to 120 (n = 2) and 40 to 60 (n = 4) min. All values have been adjusted for plasma free fraction.

where V_b is the blood volume (ml/ml). For $F_{CF} \cong 0.13$ (60–120 min) and $V_b = 0.05$, the V_T error for model 1 is 0.52 ml/ml, half of the difference between models 1 and 3.

V_T was estimated from the model that provided the best fit according to the Akaike information criterion (Akaike, 1976). In some cases, this produced an estimate of V_T with a large standard error. This was more often the case when only 60 min of bolus data was used or when the B/I studies were analyzed. Therefore, since V_T is the primary parameter of interest, the fit with the lowest *AIC* was not chosen if the standard error of V_T increased by >10% over the estimate from model 3. The model 3 estimate was used as a baseline because it had the fewest parameters and always converged. Model 3 can easily be implemented on a pixel-by-pixel basis in a similar manner to blood flow measurements (Holden et al., 1981). The same approach has been used by Koeppe et al. (1991) for pixel-by-pixel quantitation of the benzodiazepine receptor.

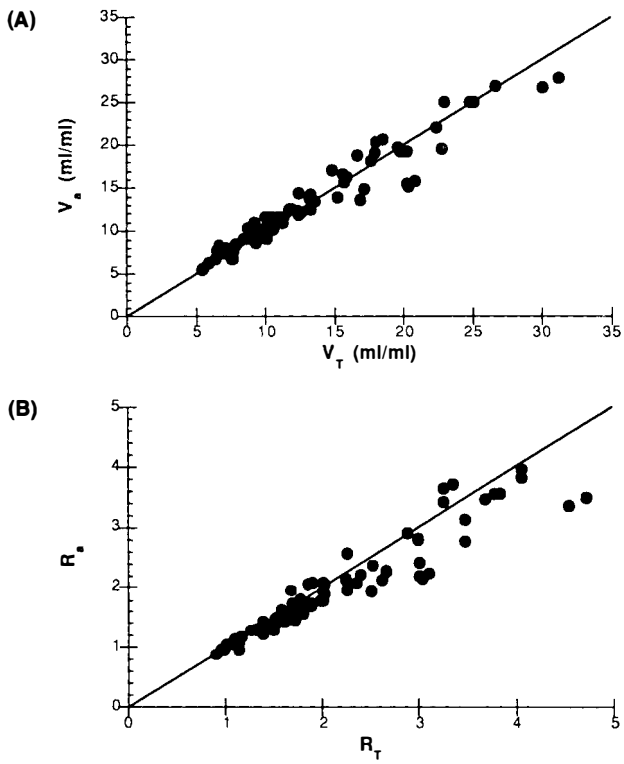

FIG. 8. A: Relationship between apparent volume of distribution (V_a) calculated from 40 to 60 min post injection and fitted value of total volume of distribution (V_T) for bolus plus continuous infusion (B/I) studies. Each data point represents 1 of 18 regions in each of four animals. Solid line is line of identity. **B:** Apparent tissue ratio values (R_a) vs. fitted values (R_T) for B/I studies. Values represent ratios of regional values to average of left and right cerebellum values. Similar results are obtained for period of 60–120 min (n = 2).

Alternatives to conventional compartment modeling

If V_T is the only parameter that is reliably estimated, it is worth considering if there are simpler data acquisition protocols or analysis schemes to measure it. With use of bolus injection data, V_T can be estimated by the ratio of the integrals to infinity of the tissue radioactivity to metabolite-corrected plasma radioactivity (Lassen and Perl, 1979). This requires extrapolation of the measured data to infinity. An interesting alternative approach is that proposed by Logan et al. (1990) whereby a data transformation produces a linear plot whose slope equals V_T. When applied to CF data, this plot reaches linearity by 10 min post injection, and estimates of the slope are in good agreement with V_T values determined from the compartmental models (data not shown). One technical issue in this method is the estimation of a slope from data when both dependent and independent variables are noisy and correlated (Beck and Arnold, 1977). This may produce small biases in the results.

Tissue ratios and transient equilibrium

The previous methods require full time-activity curves in both plasma and brain regions. As shown in Fig. 3B, a constant ratio of tissue to plasma is achieved by 60 min post injection. The time to reach

equilibrium is determined by the eigenvalues of the tissue response function (α_i; Eq. A2). Regions with high binding levels have smaller eigenvalues and require longer periods to achieve transient equilibrium, which occurs when those exponential terms have become negligible (Eq. A5). Ideally, at transient equilibrium the apparent volume of distribution (V_a) could be used as an index of receptor concentration. The derivations presented in Appendix A, the differences between V_a and V_T shown in Fig. 4A, and the dramatic change in V_a seen in the discontinued infusion study (Fig. 6D) all demonstrate that the plasma clearance rate can significantly alter the apparent volume of distribution. This results in an overestimation of V_T in all regions, with the largest errors in the regions with highest binding. If the tissue ratio R_a is used, the magnitude of error will be smaller (owing to some cancellation of errors), but will still be substantial.

Therefore, use of transient equilibrium measures produces biased estimates of V_T or R_T. These observations apply to every reversible receptor binding radiopharmaceutical. The magnitude of the bias depends upon the relative values of the tissue eigenvalues and the plasma clearance rate (β). In general, the faster the tissue clearance (larger α_1) and the slower the plasma clearance (smaller β), the smaller the inaccuracy. Also, variability in these measures will be higher owing to subject-to-subject variation in β. A further complication occurs if β is different between patient and control groups. In this case, the overestimation of V_T by V_a (or R_T by R_a) will be different between the two groups, and an incorrect conclusion concerning receptor differences between the groups may be reached. Furthermore, since these errors are smaller in regions with little specific binding, there may be little difference in the binding levels in these regions, which could inappropriately support the conclusion that measured differences in receptor-rich regions are related to receptor abnormalities. In any case, the accuracy of transient equilibrium measures should be carefully assessed by comparison with model-based values. Even if these values show a linear relationship to model-based values (as in Fig. 4), the slopes could vary across patient groups if plasma clearance rates differ.

True equilibrium by tracer infusion

A straightforward approach to eliminate the biases of transient equilibrium measures is to administer the tracer in a manner that produces true equilibrium, i.e., constant radioactivity levels in plasma and all brain compartments. Patlak and Pettigrew (1976) devised a technique for determination of an optimal infusion scheme to rapidly produce constant blood levels. This approach has been used for the measurement of the lumped constant of deoxyglucose (Sokoloff et al., 1977) and for receptor measurements (Frey et al., 1985*a*). In this study and our previous rat equilibrium study (Kawai et al., 1991), the determination of infusion schedule (Appendix B) was modified in two ways. First, the schedule was defined to bring both blood and all brain regions into equilibrium as quickly as possible, an approach previously applied to measure the distribution volume of [^{15}O]water (Carson et al., 1988*a*; Herscovitch et al., 1989). Second, since it is impractical to obtain a preliminary bolus measurement (particularly in patient studies), an infusion tailored to each individual cannot be determined. Therefore, a single infusion schedule, consisting of a B/I administration, was applied to all animals.

The results from our B/I studies are consistent with the theoretical predictions. The infusion scheme designed from the bolus data produced constant radioactivity levels in plasma and brain regions. There was good agreement between the fitted V_T values in bolus and infusion studies and also with the tissue-to-blood ratio (V_a) measured during the equilibrium period of the B/I studies. This congruence between theory and observation is in itself a validation that model-based measurements are reliable. Further studies are required to validate the physiological accuracy of the results.

The B/I administration protocol provides many advantages over bolus studies. By achieving equilibrium, V_T measurements can be performed with a single scan and a single blood sample and metabolite measurement. For more reliability, a few short scans can be acquired to verify equilibrium and a few blood samples can be analyzed. Data processing is simple and pixel-by-pixel computations are straightforward, although this can also be achieved with model 3. In human studies, the subjects need not be in the scanner during the initial phase of the study. Scanning and blood sampling are required only during the equilibrium phase and attenuation corrections can be performed using postinjection transmission scans (Carson et al., 1988*b*). The need for fewer metabolite measurements would be a significant improvement for tracers requiring HPLC determinations. For CF studies using ethyl acetate extraction, the reliability of these measurements is improved with the B/I protocol because the fraction of unmetabolized CF is higher (Fig. 6B). Also, since kinetic data are not required, scans can be acquired at interleaved axial levels to improve the spatial sampling, which is important for small receptor-rich structures. Finally, for tracers like CF that bind to

multiple receptor sites, the equilibrium approach provides an accurate measure of total binding, i.e.,

$$V_T = \omega_T(1 + K_{eq}) + \frac{B'^{(\mu)}_{max}}{K_D^{(\mu)}} + \frac{B'^{(\kappa)}_{max}}{K_D^{(\kappa)}} + V_v$$

where the superscripts refer to μ- and κ-receptor subtypes.

Infusion studies also have limitations. The B/I protocol will not produce equilibrium for subjects with significantly different blood kinetics or for regions with receptor concentrations or affinities outside the range used by the optimization procedure. As suggested above, instead of a single scan during the equilibrium period, multiple short scans (at the same or alternating anatomical levels) could be acquired to verify equilibrium. If equilibrium is satisfactory, the individual images could be averaged to improve statistical quality. In addition, if multiple blood points and metabolite measurements are taken, small residual deviations from equilibrium could be corrected. For example, with population average values for rate constants as in the fluorodeoxyglucose operational equation (Huang et al., 1980), equations such as A14 could be used to determine V_T. Such a correction would require an accurate measurement of the residual plasma clearance β. Without correction, small residual plasma clearance, randomly distributed about zero, will add to population variability. A practical disadvantage of infusions is that if there is some technical difficulty with the infusion (e.g., pump failure), the study may be lost.

Quantitation of receptors from the total volume of distribution

To estimate the binding potential (B'_{max}/K_D) from the total volume of distribution, some measure of nonspecific binding [$\omega_T(1 + K_{eq})$] is required. This could be obtained from the measured volume of distribution of a region with little or no binding (V'_T), such as cerebellum or occipital cortex. Alternatively, to properly account for regional variation in nonspecific binding levels, a paired study with the inactive enantiomer (+)-CF could be used to assess nonspecific binding region by region. A hybrid of these methods was proposed by Kawai et al. (1991), in which the nonspecific binding level is estimated by scaling V'_T by a region-specific constant, where the constant is determined from analysis of paired (+)-CF and (−)-CF studies. Finally, nonspecific binding can be assessed regionally by following the (−)-CF study with administration of the opiate antagonist naloxone to saturate all receptor sites. For the B/I infusion protocol, the (−)-CF infusion would continue while the naloxone is administered by a bolus plus infusion. Finally, to separate the binding potential into measurements of B_{max} and K_D, multiple B/I studies at different specific activities can be performed (Carson et al., 1991).

SUMMARY

Bolus injections of the opiate antagonist [^{18}F]CF produce PET data that allow reliable measurement of the total volume of distribution by conventional compartmental analysis with different models. However, individual kinetic parameters of models with two tissue compartments cannot be estimated reliably. Transient equilibrium between brain regions and plasma occurs within 60 min. The concentration ratio of tissue regions to plasma or to nonspecific tissue regions during transient equilibrium overestimates values at true equilibrium owing to plasma clearance. This effect is present to some degree for all reversible receptor binding radiopharmaceuticals and produces large errors for CF. The combination of bolus plus continuous infusion can produce true equilibrium and permits a direct measurement of the total volume of distribution. This approach may prove useful in human studies by allowing simpler protocols for scanning and blood measurements with the potential for more reliable results.

Acknowledgment: The authors express their appreciation for the excellent technical assistance of Paul Baldwin, Gerard Jacobs, Sheilah Green, William Meyer, Melvin Packer, Paul Plascjak, Norman Simpson, Stacey Stein, and Penney Yolles. The helpful suggestions of Drs. William Eckelman and Doris Doudet are gratefully acknowledged.

APPENDIX A

APPARENT VOLUME OF DISTRIBUTION V_a

This appendix presents the theory relating the apparent volume of distribution (V_a) that is achieved during transient equilibrium to the equilibrium volume of distribution (V_T).

General model

Consider an arbitrary linear compartment model with metabolite-corrected input function $C_p(t)$, impulse response function $h(t)$, and tissue concentration

$$A_T(t) = C_p(t) \otimes h(t) \qquad \text{(A1)}$$

where ⊗ is the convolution operator. The impulse response can be expressed as

$$h(t) = \sum_{j=1}^{m} A_j e^{-\alpha_j t} \quad \text{(A2)}$$

where $0 < \alpha_1 < \alpha_2 \ldots$ and where we restrict the exponents to be strictly >0, i.e., no irreversible uptake. The equilibrium volume of distribution (V_T) can be computed from Eqs. A1 and A2 by assuming a constant input function, i.e., $C_p(t) = C_0$:

$$V_T = \lim_{t\to\infty} \frac{A_T(t)}{f_p C_p(t)} = \frac{C_0 \int_0^\infty h(t)dt}{f_p C_0} = \frac{1}{f_p} \sum_{j=1}^{m} \frac{A_j}{\alpha_j} \quad \text{(A3)}$$

Now consider the case of a specific input function:

$$C_p(t) = \sum_{i=1}^{n} B_i e^{-\beta_i t} \quad \text{(A4)}$$

where $0 \leq \beta_1 < \beta_2 \ldots$. The resulting tissue function $A_T(t)$ is

$$A_T(t) = C_p(t) \otimes h(t) = \sum_{j=1}^{m} A_j \sum_{i=1}^{n} B_i \frac{e^{-\beta_i t} - e^{-\alpha_j t}}{\alpha_j - \beta_i} \quad \text{(A5)}$$

If the smallest eigenvalue of the impulse response function α_1 is larger than the smallest exponent in the input function β_1, then, beyond a certain time,

$$C_p(t) \to B_1 e^{-\beta t}$$

$$A_T(t) \to \sum_{j=1}^{m} A_j B_1 \frac{e^{-\beta t}}{\alpha_j - \beta} \quad \text{(A6)}$$

where β replaces β_1. The apparent volume of distribution approaches a constant value

$$V_a(t) = \frac{A_T(t)}{f_p C_p(t)} \to \frac{1}{f_p} \sum_{j=1}^{m} \frac{A_j}{\alpha_j - \beta} \quad \text{(A7)}$$

For a constant input function ($\beta = 0$), true equilibrium will be reached, Eq. A7 reduces to Eq. A3, and $V_a = V_T$. However, for nonequilibrium conditions ($\beta > 0$), $V_a > V_T$.

One tissue compartment

In the case of a single-tissue compartment, with influx constant K_1 and efflux constant k_2, the equilibrium volume of distribution is

$$V_T = \frac{K_1}{k_2 f_p} \quad \text{(A8)}$$

and the apparent volume of distribution from Eq. A7 reduces to

$$V_a = \frac{1}{f_p} \frac{K_1}{k_2 - \beta} \to \frac{V_T}{1 - \beta/k_2} \quad \text{(A9)}$$

If β is much smaller than k_2, then V_a will only slightly overestimate V_T. However, if β is comparable to k_2, the overestimation will be large. Note that Eq. A9 is the basis of the continuous inhalation method for cerebral blood flow (Frackowiak et al., 1980). For blood flow, instead of clearance ($\beta > 0$), the decay-corrected input function is exponentially increasing (Selikson and Eichling, 1982) with the half-life of ^{15}O ($\beta = -\ln 2/t_{1/2}$). Therefore, V_a differs from V_T and depends on flow (K_1). For receptor applications, tissue and blood data are decay corrected, and decay plays no role in transient equilibrium.

Two tissue compartments

For a model with two tissue compartments in series, the impulse response function is

$$h(t) = \frac{K_1}{\alpha_2 - \alpha_1} [(k_3 + k_4 - \alpha_1)e^{-\alpha_1 t} + (\alpha_2 - k_3 - k_4)e^{-\alpha_2 t}] \quad \text{(A10)}$$

where the eigenvalues are

$$\alpha_1 = \frac{k_2 + k_3 + k_4 - [(k_2 + k_3 + k_4)^2 - 4k_2k_4]^{1/2}}{2} \quad \text{(A11)}$$

$$\alpha_2 = \frac{k_2 + k_3 + k_4 + [(k_2 + k_3 + k_4)^2 - 4k_2k_4]^{1/2}}{2}$$

The equilibrium volume of distribution (Eq. A3) becomes

$$V_T = \frac{K_1}{k_2 f_p} \left(1 + \frac{k_3}{k_4}\right) = \frac{K_1(k_3 + k_4)}{k_2 k_4 f_p} \quad \text{(A12)}$$

where $K_1/k_2 f_p$ and $K_1 k_3/k_2 k_4 f_p$ are the volumes of distribution of free plus nonspecifically bound and specifically bound tracer, respectively. This relationship was derived more directly (Eq. 1) by setting the derivatives of the differential equations of this model to 0 and solving for $A_T/f_p C_p$. The apparent volume of distribution from Eq. A7 reduces to

$$V_a = \frac{K_1(k_3 + k_4 - \beta)}{f_p(\alpha_1 - \beta)(\alpha_2 - \beta)} \quad \text{(A13)}$$

In cases where $\beta \ll (k_3 + k_4)$ and $\beta \ll \alpha_2$, then

$$V_a \cong \frac{K_1(k_3 + k_4)}{f_p(\alpha_1 - \beta)\alpha_2} = \frac{V_T}{1 - \beta/\alpha_1} \quad \text{(A14)}$$

If β is one-half of α_1, then the apparent volume of distribution at transient equilibrium will be approximately twice the distribution volume at true equilibrium.

Tissue ratios

Suppose the ratio between a region with specific binding and a region without specific binding is of interest. If the background region can be described by a one tissue compartment model and the specific region requires a model with two tissue compartments, then the ratio at true equilibrium between these regions will be

$$R_T = \frac{V_T}{V'_T} = 1 + \frac{k_3}{k_4} \quad \text{(A15)}$$

where V'_T represents the distribution volume of the reference region and K_1/k_2 is assumed to be identical for the two regions. At transient equilibrium, the ratio will be

$$R_a = \frac{A_T(t)}{A'_T(t)} = \frac{V_a}{V'_a} = \frac{K_1(k_3 + k_4 - \beta)(k'_2 - \beta)}{K'_1(\alpha_1 - \beta)(\alpha_2 - \beta)} \quad \text{(A16)}$$

where K'_1 and k'_2 are the corresponding rate constants for the background region. The relative error in R_a (compared with R_T) will be smaller than V_a (compared with V_T) because of cancellation of some of the errors in the denominator V'_a.

APPENDIX B

DETERMINATION OF OPTIMAL INFUSION SCHEDULE

Let $f(t)$ be the time-activity curve for any brain ROI or the plasma following a bolus administration of tracer. Define an infusion protocol $H(t)$ as a combination of bolus plus continuous infusion over time T. Define the magnitude of the bolus component as K_{bol} in minutes; i.e., the bolus is equal to K_{bol} minutes worth of infusion. Therefore,

$$H(t) = \frac{K_{bol}\,\delta(t) + \theta(t) - \theta(t - T)}{K_{bol} + T} \quad \text{(B1)}$$

where $\delta(t)$ is the Dirac delta function and $\theta(t)$ is 0 for $t < 0$ and 1 for $t > 0$. $H(t)$ is normalized to 1. The predicted time-activity curve $g(t)$ in the ROI following this B/I protocol is

$$g(t) = H(t) \otimes f(t) = \frac{K_{bol} f(t) + \int_0^t f(\tau)d\tau}{K_{bol} + T} \quad \text{(B2)}$$

To choose the optimum K_{bol} value, an optimization function was defined. Choose M curves, $f_i(t)$, $i = 1, \ldots, M$, representing the range of kinetics of brain ROIs and plasma (here, plasma, thalamus, and cerebellum). These curves could be measured data or calculated from an appropriate model. Choose N time points, t_j, $j = 1, \ldots, N$, during the desired equilibrium time period (here, values equally spaced between 30 and 120 min). Using nonlinear least squares (Carson et al., 1981), choose K_{bol} to minimize the function

$$\phi = \sum_{i=1}^{M} \sum_{j=1}^{N} w_j \left[\frac{g_i(t_j)}{g_i(T)} - 1 \right]^2 \quad \text{(B3)}$$

where $g_i(t)$ is the predicted B/I curve for region i from Eq. B2, and w_j is a weight that can be used to increase the importance of the later time points. This approach minimizes the percentage difference between all curves and their final value.

REFERENCES

Akaike H (1976) An information criterion (AIC). *Math Sci* 14:5–9

Beck JV, Arnold KJ (1977) *Parameter Estimation in Engineering and Science*. New York, John Wiley & Sons

Blasberg RG, Carson RE, Kawai R, Patlak CG, Sawada Y, Channing M, Chelliah M, Herscovitch P (1989) Strategies for the study of the opiate receptor in brain: application to the opiate antagonist cyclofoxy. *J Cereb Blood Flow Metab* 9:S732

Budinger TF, Derenzo SE, Greenberg WL, Gullberg GT, Huesman RH (1978) Quantitative potentials of dynamic emission computed tomography. *J Nucl Med* 19:309–315

Burke TR, Rice KC, Pert CB (1985) Probes for narcotic receptor mediated phenomena. 11. Synthesis of 17-methyl and 17-cyclopropylmethyl-3,14-dihydroxy-4,5α-epoxy-6β-fluoromorphinans (foxy and cyclofoxy) as models of opioid ligands suitable for positron emission transaxial tomography. *Heterocycles* 23:99–106

Carson RE (1991) Precision and accuracy considerations of physiological quantitation in PET. *J Cereb Blood Flow Metab* 11:A45–A50

Carson RE, Huang SC, Phelps ME (1981) BLD—a software system for physiological data handling and model analysis. Proceedings of the Fifth Annual Symposium on Computer Applications in Medical Care, pp. 562–565

Carson RE, Braun A, Finn RD, Torregrosa J, Blasberg RG, Herscovitch P (1988*a*) Direct measurement of the distribution volume of water with positron emission tomography. *J Nucl Med* 29:822–823

Carson RE, Daube-Witherspoon ME, Green MV (1988*b*) A method for postinjection PET transmission measurements. *J Nucl Med* 29:1558–1567

Carson RE, Blasberg RG, Channing MA, Yolles PS, Dunn BB, Newman AH, Rice KC, Herscovitch P (1989) A kinetic study of the active and inactive enantiomers of ^{18}F-cyclofoxy with PET. *J Cereb Blood Flow Metab* 9:S16

Carson RE, Doudet DJ, Channing MA, Dunn BB, Der MG,

Newman AH, Rice KC, Cohen RM, Blasberg RG, Herscovitch P (1991) Equilibrium measurement of B_{max} and K_D of the opiate antagonist ^{18}F-cyclofoxy with PET: pixel-by-pixel analysis. *J Cereb Blood Flow Metab* 11:S618

Channing MA, Eckelman WC, Bennett JM, Burke TR, Rice KC (1985) Radiosynthesis of [^{18}F]3-acetylcyclofoxy: a high affinity opiate antagonist. *Intl J Appl Radiat Isot* 36:429–433

Daube-Witherspoon ME, Green MV, Holte S (1987) Performance of Scanditronix PC1024-7B PET scanner. *J Nucl Med* 28:211

Evans RD (1955) *The Atomic Nucleus*. New York, McGraw-Hill

Farde L, Hall H, Ehrin E, Sedvall G (1986) Quantitative analysis of D2 dopamine receptor binding in the living human brain by PET. *Science* 231:258–261

Farde L, Eriksson L, Blomquist G, Halldin C (1989) Kinetic analysis of central [^{11}C]raclopride binding to D_2-dopamine receptors studied by PET: a comparison to the equilibrium analysis. *J Cereb Blood Flow Metab* 9:696–708

Fenstermacher JD, Blasberg RG, Patlak CS (1981) Methods for quantifying the transport of drugs across brain barrier systems. *Pharmacol Ther* 14:217–248

Frackowiak RSJ, Lenzi GL, Jones T, Heather JD (1980) Quantitative measurement of regional cerebral blood flow and oxygen metabolism in man using ^{15}O and positron emission tomography: theory, procedure, and normal values. *J Comput Assist Tomogr* 4:727–736

Frey KA, Ehrenkaufer RLE, Beaucage S, Agranoff BW (1985*a*) Quantitative in vivo receptor binding. I. Theory and application to the muscarinic cholinergic receptor. *J Neurosci* 5:421–428

Frey KA, Hichwa RD, Ehrenkaufer RLE, Agranoff BW (1985*b*) Quantitative in vivo receptor binding. III. Tracer kinetic modeling of muscarinic cholinergic receptor binding. *Proc Natl Acad Sci USA* 82:6711–6715

Frost JJ, Douglass DH, Mayberg HS, Dannals RF, Links JM, Wilson AA, Ravert HT, Crozier WC, Wagner HN (1989) Multicompartmental analysis of [^{11}C]carfentanil binding to opiate receptors in humans measured by positron emission tomography. *J Cereb Blood Flow Metab* 9:398–409

Herscovitch P, Carson RE, Berg GW, Daube-Witherspoon ME, Jacobs GI (1989) A method for rapid equilibration between brain and blood: application to the measurement of the partition coefficient of water with PET. *J Cereb Blood Flow Metab* 9:S240

Hoffman EJ, Huang SC, Phelps ME (1979) Quantitation in positron emission computed tomography: 1. Effect of object size. *J Comput Assist Tomogr* 3:299–308

Holden JE, Gatley SJ, Hichwa RD, Ip WR, Shaughnessy WJ, Nickles RJ, Polcyn RE (1981) Cerebral blood flow using PET measurements of fluoromethane kinetics. *J Nucl Med* 22:1084–1088

Huang SC, Phelps ME (1986) Principles of tracer kinetic modeling in positron emission tomography and autoradiography. In: *Positron Emission Tomography and Autoradiography: Principles and Applications for the Brain and Heart* (Phelps M, Mazziotta J, Schelbert H, eds), New York, Raven Press, pp 287–346

Huang SC, Phelps ME, Hoffman EJ, Sideris K, Selin CJ, Kuhl DR (1980) Non-invasive determination of local cerebral metabolic rate of glucose in man. *Am J Physiol* 238:E69–E82

Huang SC, Barrio JR, Phelps ME (1986) Neuroreceptor assay with positron emission tomography. *J Cereb Blood Flow Metab* 6:515–521

Huang SC, Bahn MM, Barrio JR, Hoffman JM, Satyamurthy N, Hawkins RA, Mazziotta JC, Phelps ME (1989) A double injection technique for in vivo measurement of dopamine D_2-receptor density in monkeys with 3-(2-[^{18}F]fluoroethyl)spiperone and dynamic positron emission tomography. *J Cereb Blood Flow Metab* 9:850–858

Kawai R, Sawada Y, Channing M, Dunn B, Newman AH, Rice KC, Blasberg RG (1990*a*) Kinetic analysis of the opiate antagonist cyclofoxy in rat brain: simultaneous infusion of active and inactive enantiomers. *J Pharmacol Exp Ther* 255: 826–835

Kawai R, Sawada Y, Channing M, Newman AH, Rice KC, Blasberg RG (1990*b*) BBB transport and rapid tissue binding of the opiate antagonist cyclofoxy: comparison of active and inactive enantiomers. *Am J Physiol* 259:H1278–H1287

Kawai R, Carson RE, Dunn B, Newman AH, Rice KC, Blasberg RG (1991) Regional brain measurement of B_{max} and K_D with the opiate antagonist cyclofoxy: equilibrium studies in the conscious rat. *J Cereb Blood Flow Metab* 11:529–544

Kessler RM, Ellis JR, Eden M (1984) Analysis of emission tomographic scan data: limitations imposed by resolution and background. *J Comput Assist Tomogr* 8:514–522

Koeppe RA, Holthoff VA, Frey KA, Kilbourn MR, Kuhl DE (1991) Compartmental analysis of [^{11}C]flumazenil kinetic for the estimation of ligand transport rate and receptor distribution using positron emission tomography. *J Cereb Blood Flow Metab* 11:735–744

Lassen NA, Perl W (1979) *Tracer Kinetic Methods in Medical Physiology*. New York, Raven Press

Lewis ME, Mishkin M, Bragin E, Brown RM, Pert CB, Pert A (1981) Opiate receptor gradients in monkey cerebral cortex: correspondence with sensory processing hierarchies. *Science* 211:1166–1169

Logan J, Wolf AP, Shiue CY, Fowler JS (1987) Kinetic modeling of receptor-ligand binding applied to positron emission tomographic studies with neuroleptic tracers. *J Neurochem* 48:73–83

Logan J, Fowler JS, Volkow ND, Wolf AP, Dewey SL, Schyler DJ, MacGregor RR, Hitzemann R, Bendriem B, Gatley SJ, Christman D (1990) Graphical analysis of reversible radioligand binding from time-activity measurements applied to [*N*-^{11}C-methyl]-(−)-cocaine: PET studies in human subjects. *J Cereb Blood Flow Metab* 10:740–747

Mintun MA, Raichle ME, Kilbourn MR, Wooten GF, Welch MJ (1984) A quantitative model for the in vivo assessment of drug binding sites with positron emission tomography. *Ann Neurol* 15:217–227

Ostrowski NL, Burke TRJ, Rice KC, Pert A, Pert CB (1987) The pattern of [^{3}H]cyclofoxy retention in rat brain after in vivo injection corresponds to the in vitro opiate receptor distribution. *Brain Res* 402:275–286

Patlak CS, Pettigrew KD (1976) A method to obtain infusion schedules for prescribed blood concentration time courses. *J Appl Physiol* 10:458–463

Perlmutter JS, Larson KB, Raichle ME, Markham J, Mintun MA, Kilbourn MR, Welch MJ (1986) Strategies for in vivo measurement of receptor binding using positron emission tomography. *J Cereb Blood Flow Metab* 6:154–169

Pert CB, Danks JA, Channing MA, Eckelman WC, Larson SM, Bennett JM, Burke TRJ, Rice KC (1984) 3-[^{18}F]Acetylcyclofoxy: a useful probe for the visualization of opiate receptors in living animals. *FEBS Lett* 177:281–286

Riche D, Hantraye P, Guibert B, Naquet R, Loc'h C, Maziere B, Maziere M (1988) Anatomical atlas of the baboon's brain in the orbito-meatal plane used in experimental positron emission tomography. *Brain Res Bull* 20:283–301

Rothman RB, McLean S (1988) An examination of the opiate receptor subtypes labeled by [^{3}H]cyclofoxy: an opiate antagonist suitable for positron emission tomography. *Biol Psychiatry* 23:435–458

Rothman RB, Bykov V, Reid A, De Costa BR, Newman AH, Jacobson AE, Rice KC (1988) A brief study of the selectivity of norinaltorphimine, (−)-cyclofoxy and (+)-cyclofoxy among opioid receptor subtypes in vitro. *Neuropeptides* 12: 181–187

Sadzot B, Price JC, Mayberg HS, Douglass KH, Dannals RF, Lever JR, Ravert HT, Wilson AA, Wagner HNJ, Feldman MA, Frost JJ (1991) Quantification of human opiate receptor concentration and affinity using high and low specific activity [^{11}C]diprenorphine and positron emission tomography. *J Cereb Blood Flow Metab* 11:204–219

Salmon E, Brooks DJ, Leenders KL, Turton DR, Hume SP,

Cremer JE, Jones T, Frackowiak RSJ (1990) A two-compartment description and kinetic procedure for measuring regional cerebral [^{11}C]nomifensine uptake using positron emission tomography. *J Cereb Blood Flow Metab* 10:307–316

Sawada Y, Hiraga S, Patlak CS, Ito K, Pettigrew KD, Blasberg RG (1990) Cerebrovascular transport of ^{125}I-quinuclidinyl benzilate, ^{3}H-cyclofoxy, and ^{14}C-iodoantipyrine. *Am J Physiol* 258:H1585–H1598

Sawada Y, Kawai R, McManaway M, Otsuki H, Rice KC, Patlak CS, Blasberg RG (1991) Kinetic analysis of transport and opioid receptor binding of [^{3}H]cyclofoxy in rat brain in vivo: implications for human studies. *J Cereb Blood Flow Metab* 11:183–203

Selikson N, Eichling J (1982) Continuous administration of short-lived isotopes for evaluating dynamic parameters. *Phys Med Biol* 27:1381–1392

Sokoloff L, Reivich M, Kennedy C, des Rosiers MH, Patlak CS, Pettigrew KD, Sakurada O, Shinohara M (1977) The [^{14}C]deoxyglucose method for the measurement of local cerebral glucose utilization: theory, procedure, and normal values in the conscious and anesthetized albino rat. *J Neurochem* 28:897–916

Wong DR, Gjedde A, Wagner HM (1986*a*) Quantification of neuroreceptors in the living human brain. I. Irreversible binding of ligands. *J Cereb Blood Flow Metab* 6:137–146

Wong DR, Gjedde A, Wagner HM, Dannals RF, Douglass KH, Links JM, Kuhar MJ (1986*b*) Quantification of neuroreceptors in the living human brain. II. Inhibition studies of receptor density and affinity. *J Cereb Blood Flow Metab* 6: 147–153